CHARLES UNIVERSITY IN PRAGUE

Faculty of Science

Physical & Macromolecular Chemistry

Bachelor thesis

Reliability of DFT methods for the description of electronically excited states of copper ions

Lukáš Grajciar

2007

Advisor: Doc. RNDr. Petr Nachtigall, Ph.D.

INSTITUTE OF ORGANIC CHEMISTRY AND BIOCHEMISTRY

Center for Complex Molecular Systems and Biomolecules

I declare that I worked out this thesis solely by myself, using the cited references.

Prague, 30.05.2007 Lukáš Grajciar

I would like to thank Dr. Peter Nachtigall for his kind guidance, support and patience as well as my parents for their support during my studies.

Contents

The list of abbreviations 5

1 Introduction 6

2 Methods 8

2.1 The Hartree – Fock approximation 8
2.2 Coupled clusters method (CC) 9
2.3 Averaged quadratic coupled clusters method (AQCC) 10
2.4 Density functional theory (DFT) 11
2.5 The generalized model of the vertical transition energy 13

3 Calculations 16

4 Results 18

4.1 $Cu^{+}(H_2O)_N$ model systems 18
4.2 Vertical excitation energies of model systems 21
4.3 Vertical excitation energies in ZSM-5 zeolite 22

5. Discussion 24

5.1 CCSD(T) vs. B3LYP 24
5.2 CCSD(T) vs. PBE 25
5.3 B3LYP vs. PBE 25
5.4 CCSD(T) vs. AQCC 25
5.5 Dependence of vertical excitation energy on the system size 26
5.6 The ZSM-5 zeolite vs. cluster model vertical excitation energies 27

7. Conclusions 29

Reference List 31

The list of abbreviations

ACPF	Averaged Coupled-Pair Functional
AQCC	Averaged Quadratic Coupled Clusters
B	Becke Functional
B3LYP	hybrid exchange-correlation functional using B and LYP
CC	Coupled Clusters
CCD	Coupled Clusters Doubles
CCSD	Coupled Clusters Singles and Doubles
CCSDT	Coupled Clusters Singles, Doubles and Triples
CCSD(T)	Coupled Clusters Singles, Doubles; Triplets calculated with perturbation theory
CEPA	Coupled Electron-Pair Approximation
CI	Configuration Interaction
CISD	Configuration Interaction Singles and Doubles
DFT	Density Functional Theory
DFT/B3LYP	Density Functional Theory employing B3LYP hybrid functional
DFT/PBE	Density Functional Theory employing PBE functional MP2 Møller-Plesset Perturbation Theory up to the second order
EPR	Electron Paramagnetic Resonance
EXAFS	Extended X-ray Absorption Fine Structure
FTIR	Fourier-Transform Infrared Spectroscopy
GGA	Generalized Gradient Approximation
HF	Hartree-Fock
MCSCF	Multi-Configurational Self-Consistent Field
MR-AQCC	Multi-Reference Averaged Quadratic Coupled Cluster
LCCD	Linearized Coupled Cluster Doubles
LDA	Local Density Approximation
LYP	Lee-Yang-Parr functional
PBE	Perdew-Burke-Ernzerhof functional
XANES	X-ray Absorption Near Edge Structure

1 Introduction

In order to investigate the electron structure of many-body systems we need to solve the stationary Schrödinger equation. Different approaches for solving the stationary Schrödinger equation have been developed, e.g., Hartree-Fock (HF) method, post-HF methods and density functional theory (DFT). The HF and post-HF methods are well established methods with an advantage of being systematically improvable but often at an expense of high computational demands. The density functional theory represents a rather different approach. While the HF is a wave-function based approach the DFT introduces an electron density as a quantity fully determining the electron structure and resulting properties. The main advantage of this approach is the simplicity of having a function of just three variables instead of function depending on $3N$ variable. It is important to note though that the values of the studied properties obtained using the DFT needs to be compared to more accurate methods (CCSD(T), MP2) as the exact form of the terms involving the exchange and correlation interactions is not known (see paragraph 2.4). Still the computational simplicity which allows for the calculations of large systems and the improving quality of the approximations of exchange-correlation functionals makes the DFT one of the most popular methods for the electronic structure calculations.

One of such a large systems are zeolites – alumino-silicate minerals with an "open" structure that can accommodate a wide variety of cations (Na^+, Ca^{2+}, Cu^+ etc.) that are coordinatively unsaturated and can be exchanged for the other cations in a contact solution. Specifically, the Cu^+ cation exchanged zeolite ZSM-5 exhibits high activity for the catalytic decomposition of NO and for the selective catalytic reduction of NO by C_3 and C_4 hydrocarbons in an excess of oxygen.[1-3] It is proposed that the coordination of Cu^+ cation to the zeolite framework plays the major role in a catalytic activities of the zeolite. In order to predict the possible coordination sites for Cu^+ cation in ZSM-5, theoretical studies have been carried out[4,5] using various methods, including DFT. In order to interpret the values obtained from the DFT calculations correctly the comparison with a more established method and/or experimental data is required. In the

case of zeolites experimental data typically include various spectroscopic techniques, e.g., FTIR, EXAFS, XANES, EPR and UV-Vis.[6-9]

The present study aims to check the reliability of the DFT method employing different functionals (PBE, B3LYP) for the description of electronically excited states of copper ions by comparing it with both a more accurate method (CCSD(T)) and an experiment. The property chosen for the study was the vertical excitation energy as there is a possibility for a direct comparison with the experimental data obtained from the excitation photoluminiscence spectra.[9]

2 Methods

2.1 The Hartree – Fock approximation

The HF approximation is used to solve the time-independent Schrödinger equation for a many-electron system. The essence of this approach is to replace the many-electron problem by one-electron problem using the model of independent electrons. This aim is reached by the introduction of the full electronic molecular Hamiltonian as a sum of the one-electron Fock operators and by expressing the many-electron wave function as a Slater determinant:

$$\Psi(x_1, x_2, ..., x_N) = (N!)^{-1/2} \begin{vmatrix} \chi_1(x_1) & \chi_2(x_1) & \cdots & \chi_N(x_1) \\ \chi_1(x_2) & \chi_2(x_2) & \cdots & \chi_N(x_2) \\ \vdots & \vdots & \ddots & \vdots \\ \chi_1(x_N) & \chi_2(x_N) & \cdots & \chi_N(x_N) \end{vmatrix} \quad (1)$$

where the N is the total number of electrons and $\chi_i(x_i)$ is a *i*th spin-orbital (the one-electron wave function). occupied by the *i*th electron The Fock operator is of a form:

$$\hat{f}_i = -\frac{1}{2}\Delta_i - \sum_{A=1}^{M} \frac{Z_A}{r_{iA}} + v_i \quad (2)$$

where Z_A is charge of nucleus, r_{iA} is distance between electron and nucleus, Δ_i is a Laplacian operator and v_i is the average potential experienced by the *i*th electron as the result of the presence of the other electrons. This is also known as a mean field approximation. Thus, the correlated motion of an electron with every other electron is ignored. The neglection of the electron correlation is a major drawback of the HF approximation. The qualitative description of the electron correlation is connected with the term of correlation energy, E_{corr}, defined as the difference between the exact nonrelativistic energy of the system E_0 and the HF-limit energy E^{HF}(the HF energy obtained with the complete basis set):

$$E_{corr} = E_0 - E^{HF} \quad (3)$$

The HF method is variational, thus, the HF energy is an upper bound to the exact energy and, thus, the correlation energy is negative.

A number of approaches have been devised to include electron correlation to the many-electron wave function. These are called the post-HF methods – such as Møller-Plesset Perturbation Theory[10], Configuration Interaction and Coupled Clusters. But the HF approximation still remains the starting point for these more accurate methods. An approach bypassing the HF approximation used in some cases is a density functional theory, which gives approximate solutions to both, exchange and correlation energies.

2.2 Coupled clusters method (CC)

Coupled clusters method[11] is a numerical technique starting from the HF method and adding a correction term to take into account the electron correlation. The central idea is that the exact nonrelativistic ground-state molecular electronic wave function Ψ can be described as follows:

$$\Psi = \hat{e}^T \Phi_0 \tag{4}$$

where Φ_0 is the normalized ground-state HF wave function and the operator $\hat{e}^T$ is defined as the Taylor-series expansion:

$$\hat{e}^T = 1 + \hat{T} + \frac{\hat{T}^2}{2!} + ... = \sum_{k=0}^{\infty} \frac{\hat{T}^k}{k!} \tag{5}$$

and the cluster operator $\hat{T}$ is

$$\hat{T} = \hat{T}_1 + \hat{T}_2 + ... + \hat{T}_n \tag{6}$$

where n is the number of electrons in the molecule and the $\hat{T}_i$ operators generate all possible determinants having i excitation from the reference, *e.g.* ,

$$\hat{T}_1 \Phi_0 = \sum_{a=n+1}^{\infty} \sum_{i=1}^{n} t_i^a \Phi_i^a \tag{7}$$

where Φ_i^a is a singly excited Slater determinant (see (1)) with occupied spin-orbital χ_i replaced by the virtual spin-orbital χ_a and t_i^a are the coefficients (amplitudes). Hence, the Ψ is expressed as a linear combination of Slater determinants that include Φ_0 and all possible excitation of electrons from occupied to virtual spin-orbitals. This is in essence the full CI. The advantage of CC is that the method is size consistent even if the cluster

operator $\hat{T}$ (see (6)) is truncated. In order to sustain the computational feasibility the $\hat{T}$ operator needs to be truncated. The coupled-cluster methods are classified according to the extent of the truncation:

CCD (coupled-clusters doubles) - $\hat{T} = \hat{T}_2$

CCSD (coupled-clusters singles and doubles) - $\hat{T} = \hat{T}_1 + \hat{T}_2$

CCSDT (coupled-clusters singles, doubles and triples) - $\hat{T} = \hat{T}_1 + \hat{T}_2 + \hat{T}_3$

the scaling behavior of CCSD is on the order of N^6 while CCSDT scales as N^8, making it almost intractable except for the small molecules. The excellent compromise between the accuracy and the cost poses a CCSD(T) method, where the T in the parenthesis indicates that the triples are calculated within the perturbation theory. CCSD(T) is often referred as a gold-standard level of theory for the single-reference calculations. That is why it was chosen as a benchmark method in our study. It is important to note that the standard implementation cannot be used for the excited states.

2.3 Averaged quadratic coupled clusters method (AQCC)

The aim of a CC calculation is to find the values of the amplitudes $t_i^a, t_{ij}^{ab}, \ldots$ for all *i, j, ...,* and all *a, b, ...* in order to obtain the wave function Ψ. This aim is accomplished in the CCD approximation by solving a set of simultaneous nonlinear equations for the unknown amplitudes in the following form:

$$\sum_{s=1}^{m} a_{rs} x_s + \sum_{t=2}^{m} \sum_{s=1}^{t-1} b_{rst} x_s x_t + c_r = 0, \qquad r = 1,2,\ldots,m \tag{8}$$

where $x_1, x_2, \ldots, x_m$ are the unknowns t_{ij}^{ab}, the quantities a_{rs}, b_{rst}, and c_r are constants and m is the number of unknown amplitudes t_{ij}^{ab}. Several approximations to the CCD method have been developed (CEPA, LCCD, ACPF).[12-16]

The AQCC method, considered as size-extensively corrected CISD procedure, includes the quadratic (EPV) terms, *e.g.* , $x_s x_t$ from (7), in an averaged way. The AQCC method offers a similar performance as the CCSD(T) method. The multi-reference variant of AQCC has been also developed (denoted as MR-AQCC).[17] Although the MR-

AQCC has been used mainly for calculations of the electronic ground state of a given symmetry, the computation of the excited states is also possible.[18]

2.4 Density functional theory (DFT)

While the HF is based on many-electron wave function depending on $3N$ variables (three spatial variables for each of the N electrons) the DFT[19,20] replaces the many-electron wave function with the electronic density ρ which is a function of only three variables:

$$\rho(\vec{r}_1) = N \int d^3 r_2 \int d^3 r_3 \ldots \int d^3 r_N \Psi^*(\vec{r}_1, \vec{r}_2, \ldots, \vec{r}_N)\Psi(\vec{r}_1, \vec{r}_2, \ldots, \vec{r}_N) \qquad (9)$$

where N is the number of electrons and Ψ is N electron wave function. The possibility of replacing the many-electron wave function with the electronic density is justified by two Hohenberg-Kohn theorems.[20] The first one proves that the ground-state electron properties (wave function, energy, *etc.*) are uniquely determined by the electron density and the second one shows that the density obeys the variational principle. The energy functional of the system is as follows (within the Born-Oppenheimer approximation):

$$E[\rho(\vec{r})] = T_{ni}[\rho(\vec{r})] + V_{ne}[\rho(\vec{r})] + V_{ee}[\rho(\vec{r})] + \Delta T[\rho(\vec{r})] + \Delta V_{ee}[\rho(\vec{r})] \qquad (10)$$

where the energy funtionals on the right hand side refer, respectively, to the kinetic energy of the non-interacting electrons, the nuclear-electron interaction, the classical electron-electron repulsion, the correction to the kinetic energy deriving from the interacting nature of the electrons, and all the non-classical corrections to the electron-electron repulsion energy - exchange and correlation interaction along with the correction for the classical self-interaction. While the exact form of the first three terms are known that is not the case for the last two terms, also referred as exchange correlation functional $E_{xc}[\rho(\vec{r})]$:

$$E_{xc}[\rho(\vec{r})] = \int \rho(\vec{r}) \varepsilon_{xc}[\rho(\vec{r})] d\vec{r} \qquad (11)$$

where ε_{xc} is the energy density per particle density. Finding the correct form of the exchange correlation functional represents a major problem of the DFT approach. Few approximation for finding the form of exchange correlation functional have been adopted.

The most widely used is the Local density approximation (LDA), where the functional depends only on the energy density at the coordinate where the functional is evaluated.

Another way to improve the exchange correlation functional is to make it dependent not only on the local value of the energy density but on the gradient of the energy density at the coordinate where the functional is evaluated – generalized gradient approximation (GGA). The GGA exchange functional of Perdew-Burke-Ernzerhof (PBE)[21,22] was one of the DFT functionals chosen for this study as it is widely used in solid state calculations (*e.g.*, zeolites).

The second functional used is the hybrid exchange correlation functional B3LYP[23] based on the adiabatic connection method (ACM) in which the exchange part of the functional is a combination of the Becke's (B) exchange GGA functional[24] and the exact exchange energy from Hartree-Fock theory while the Lee-Yang-Parr (LYP)[25] correlation GGA functional is used for the correlation part. The form of the B3LYP hybrid functional is defined by three parameters, specifying how much of the exact exchange is mixed in. The B3LYP has proven the most popular functional to date thanks to its remarkably good performance across wide variety of applications in chemistry.

Although the results obtained with these functionals are usually sufficiently accurate for most applications, it is well known that there is no systematical way in DFT to improve its results as in the conventional *ab initio* theory. Hence, it is not possible to estimate the error of the DFT calculations without comparing them to other more accurate methods or experiment. The comparison with more accurate methods or experiment also enable us to choose the optimal functional for a particular case of application, *e.g.*, the calculation of vertical excitation energies as discussed later. On the other hand the DFT is due to its computational simplicity (it scales no worse than N^3) used for the computation on the large systems.

The validity of the Hohenberg-Kohn theorems can be extended to the lowest energy (non-degenerate) state within each irreducible representation of the molecular point group; however, the extension to the higher energy excited states is problematic. In order to compute the excited states different approach is needed – Time-dependent DFT.

2.5 The generalized model of the vertical transition energy.

By absorbing the photon the molecule is lifted from the ground-state to the excited state. The consequent distribution of the absorbed quantum resulting from both radiative (1-3 in Figure 1) and non-radiative (4-6 in Figure 1) transitons is depicted on generalized Jablonski diagram (Figure 1).

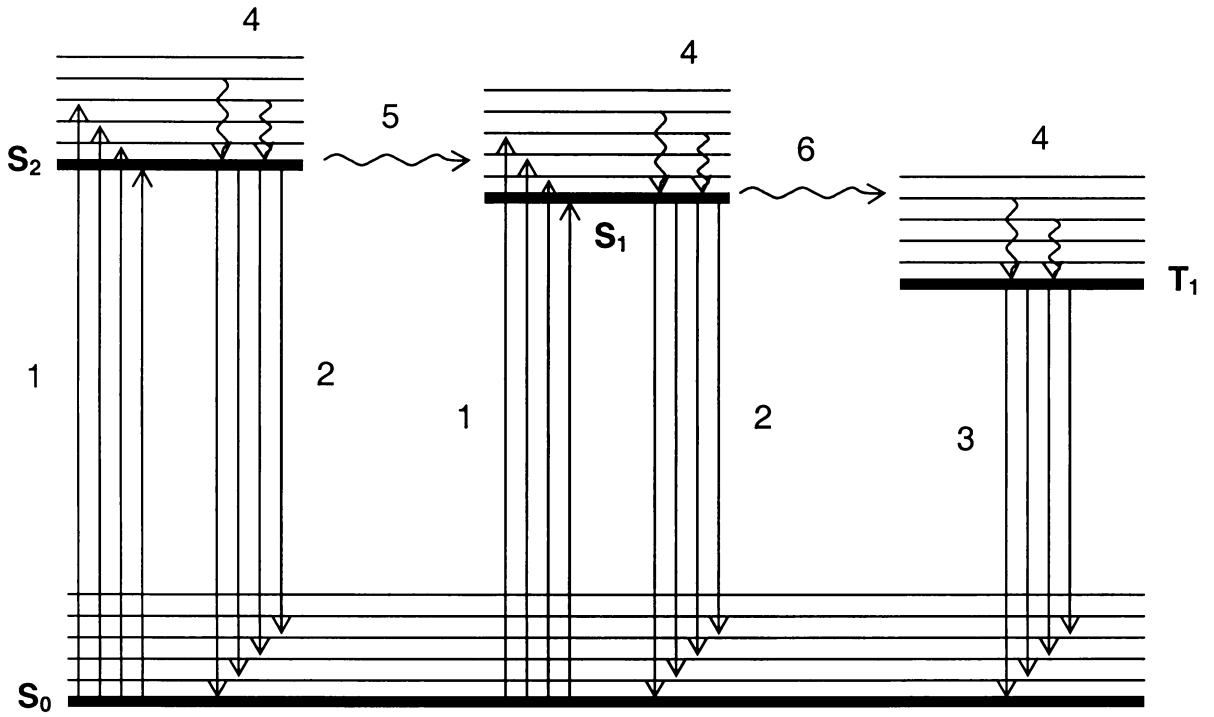

Figure 1. Generalized Jablonski diagram. Bold horizontal lines represent the electronic states while the thin horizontal lines represent the corresponding vibrational states. 1 – absorption, 2 – fluorescence, 3 – phosphorescence, 4 – vibrational relaxation, 5 – internal conversion, 6 – intersystem crossing.

As it can be seen from the Jablonski diagram a couple of vibronic (simultaneous changes in electronic and vibrational energy levels) transitions from the ground to the excited state can occur. The intensity of the vibronic transition corresponding to the probability of the transition is explained by Franck-Condon principle. It states that since electronic transitions are very fast compared with nuclear motions, vibrational levels are favored when they correspond to a minimal change in the nuclear coordinates. The state resulting from the most favored vibronic transition is called a Franck–Condon state, and the transition involved, a vertical transition (Figure 2).

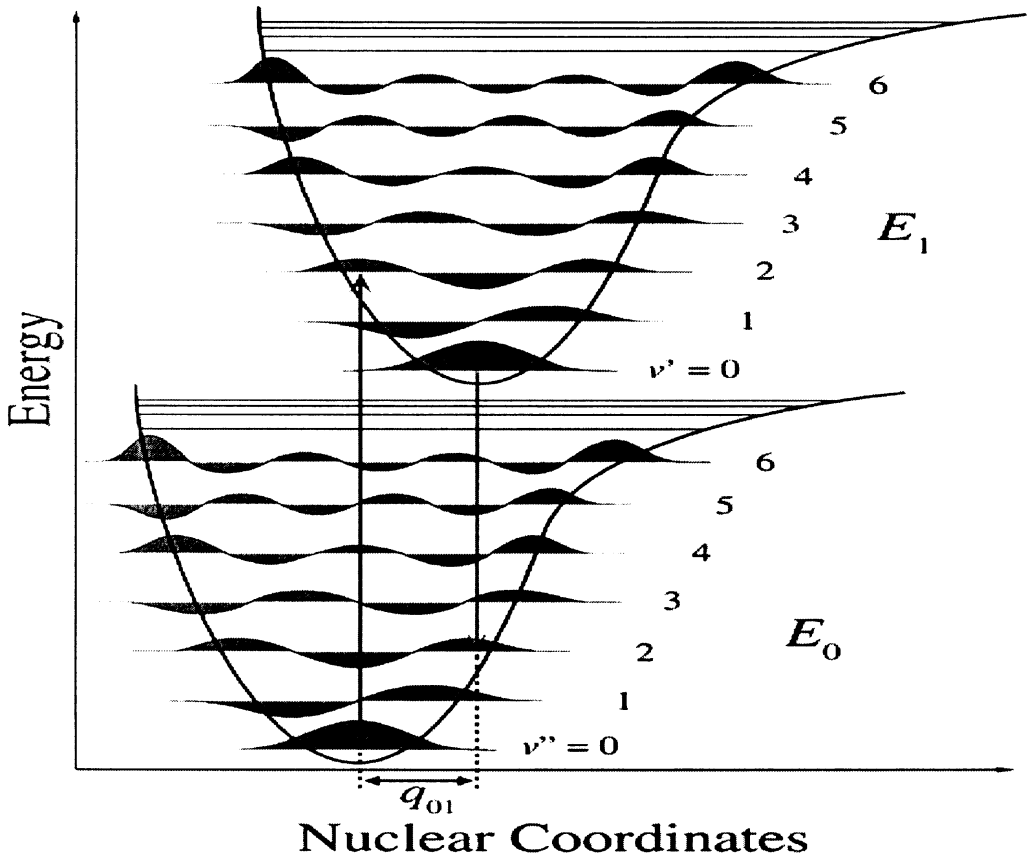

Figure 2. Franck-Condon principle energy diagram. The energy change marked out by the dark gray vertical line with an arrow represents the vertical excitation energy while the one marked by the gray vertical line represents the vertical emission energy (fluorescence). q_{01} is a change in nuclear coordinates associated with the relaxation of the system in excited state.

Thus, the maxima in the absorption spectra can be assigned to the vertical $E_1 \leftarrow E_0$ transition and maxima in the emission spectra to the vertical $E_0 \leftarrow E_1$ transition. The energy change corresponding to the vertical $E_1 \leftarrow E_0$ transition is called the vertical excitation energy while the energy change corresponding to the vertical $E_0 \leftarrow E_1$ transition is called the vertical emission energy. It's important to note that the transition between states with different multiplicity is far less probable and thus far less intensive (forbidden) than the transition between the states with the same multiplicity.

In our study the vertical $T_1 \leftarrow S_0$ and $S_1 \leftarrow S_0$ excitation energies are computed. We confine ourselves to the lowest-energy states within a given multiplicity and irreducible representation. This is due to the previously discussed incapability of both CCSD(T) and

DFT to treat the excited states unless a special approach is adopted (time-dependent DFT, equation-of-motion coupled cluster, multi-reference coupled cluster).[26-29]

3 Calculations

Various computational approaches have been adopted in the present study. The geometry optimization of the singlet ground state was carried out using DFT approach employing the B3LYP exchange-correlation functional.

The basis set used includes the (62111111s/33111p/311d) valence basis set augmented by one p function with exponent 0.155 (Ahlrichs VTZ+1p) on Cu atom[30] and the correlation consistent valence double-ζ-plus-polarization basis set (cc-pVDZ) on H and O atoms[31] (this basis set will be denoted as GO-BS throughout the text).

Four different model systems were optimized under the symmetry constrains specified in Table 1.

Table 1. Symmetry groups assigned to the $Cu^+(H_2O)_n$ systems.

Symmetry	$Cu^+(H_2O)_2 - C_{2v}$	$Cu^+(H_2O)_2 - D_{2h}$	$Cu^+(H_2O)_3 - C_{2v}$	$Cu^+(H_2O)_4 - D_{2h}$
Geometry optimalization	C_{2v}	D_{2h}	D_{3h}	D_{4h}
Vertical energy computation[a]	C_{2v}	D_{2h}	C_{2v}	D_{2h}

[a] Symmetry point groups used for the vertical energy computation are the largest Abelian subgroups corresponding to the point group of the cluster model. This restriction is due to software incapability to treat a non-Abelian point groups.

The optimized structures of the model systems were used in single-point vertical excitation energies calculations. The $T_1 \leftarrow S_0$ vertical excitation energies were calculated at both the DFT (using both B3LYP and PBE exchange-correlation functionals) and AQCC level while $S_1 \leftarrow S_0$ vertical excitation energies were calculated only at the AQCC level. In addition, lowest energy triplet state in each irreducible representation along with the ground state singlet were calculated at the CCSD(T) level of theory. The AQCC method was preceded with MCSCF calculations in order to generate reference wave functions for both $T_1 \leftarrow S_0$ and $S_1 \leftarrow S_0$ AQCC vertical excitation energies calculations. The CCSD(T) was chosen as a benchmark method for the prior calculations.

The basis set used for the vertical excitation energy computation includes the energy-adjusted relativistic effective core pseudopotential and a (311111s/22111p/

411d/11f/1g) valence polarization basis set (Stuttgart RSC 1997 ECP + 2f1g) on Cu atom[32] and the correlation consistent valence quadruple-ζ-plus-polarization basis set (cc-pVQZ) on O and H atoms[31] (this basis set will be denoted as VE-BS throughout the text).

Since we use the valence basis sets the correct description of the electron correlation of the core orbitals is not possible. Hence, not all the orbitals were correlated in CCSD(T), AQCC and MCSCF. The chosen core orbitals correspond to 3s and 3p Cu orbitals (1s,2s and 2p orbitals of Cu are contained in pseudopotential) and 1s O orbitals (more accurately as a symmetry-adapted linear combinations). The usage of this approximation is a consequence of the fact that although the contribution of the core orbitals to the correlation energy is significant it is almost the same for the studied changes in the valence ("chemical") space.

As for the active space definition in AQCC and MCSCF, the Cu(4s) orbital and the highest Cu(3d) orbital of corresponding symmetry were considered.

The geometry optimization and the vertical excitation energy calculations have been carried out with the use of Gaussian03[33] and MOLPRO02[34] software packages, respectively.

4 Results

4.1 $Cu^{+}(H_20)_n$ model systems

In order to check the reliability of the DFT method for the description of electronically excited states of copper ions, four model systems containing Cu^{+} ion and 2, 3 or 4 molecules of water were considered: $Cu^{+}(H_2O)_2$ – C_{2v}, $Cu^{+}(H_2O)_2$ – D_{2h}, $Cu^{+}(H_2O)_3$ – C_{2v}, $Cu^{+}(H_2O)_4$ – D_{2h}, where the symbols after dash denote the largest concise Abelian group assigned to symmetry point group of computed systems. The systems were, as previously discussed, optimized in a singlet state (see Figures 3-6 for optimized structures) making use of corresponding symmetry constrains. In case of $Cu^{+}(H_2O)_2$ – C_{2v}, all parameters except the O-Cu-O angle were optimized while the O-Cu-O angle was taken from preliminary AlO_4H_8 (1-T) model optimalization.[35]

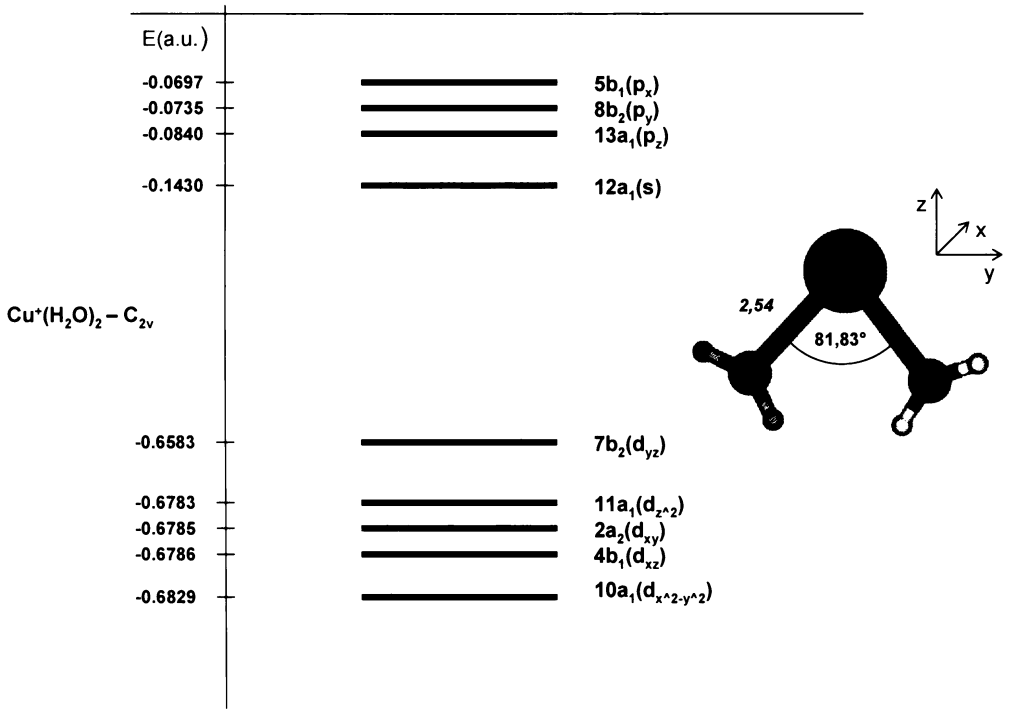

Figure 3. HF orbital diagram with the corresponding irreducible representation assignments and orbital energies, the singlet-optimized structures of cluster model $Cu^{+}(H_2O)_2$-C_{2v}

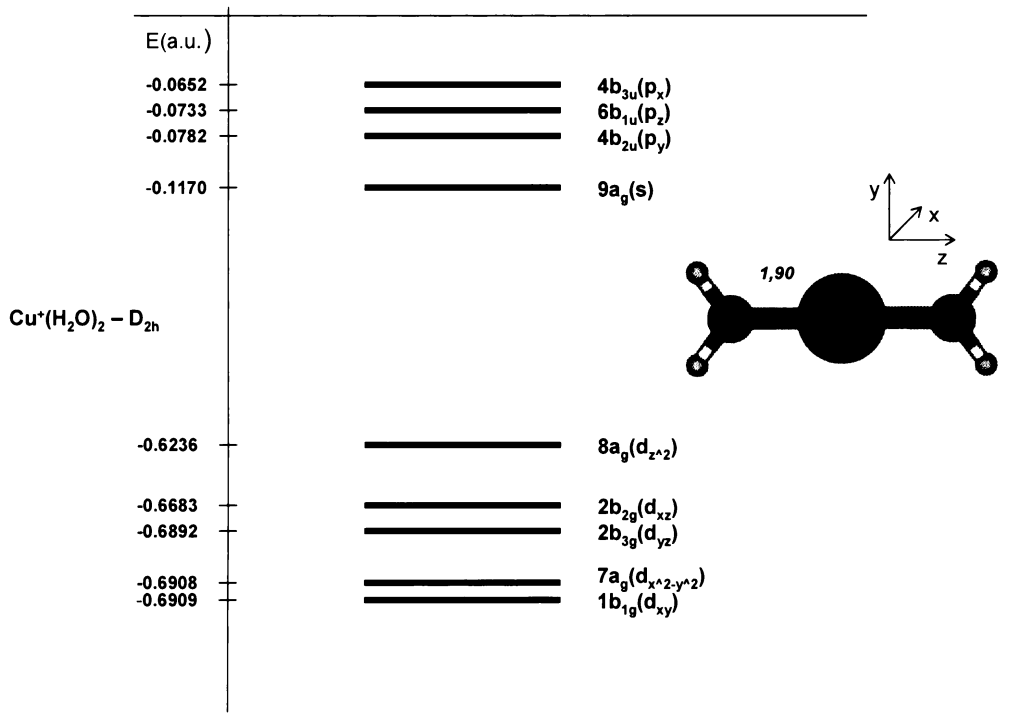

Figure 4. HF orbital diagram with the corresponding irreducible representation assignments and orbital energies, the singlet-optimized structures of cluster model $Cu^{+}(H_2O)_2$-D_{2h}.

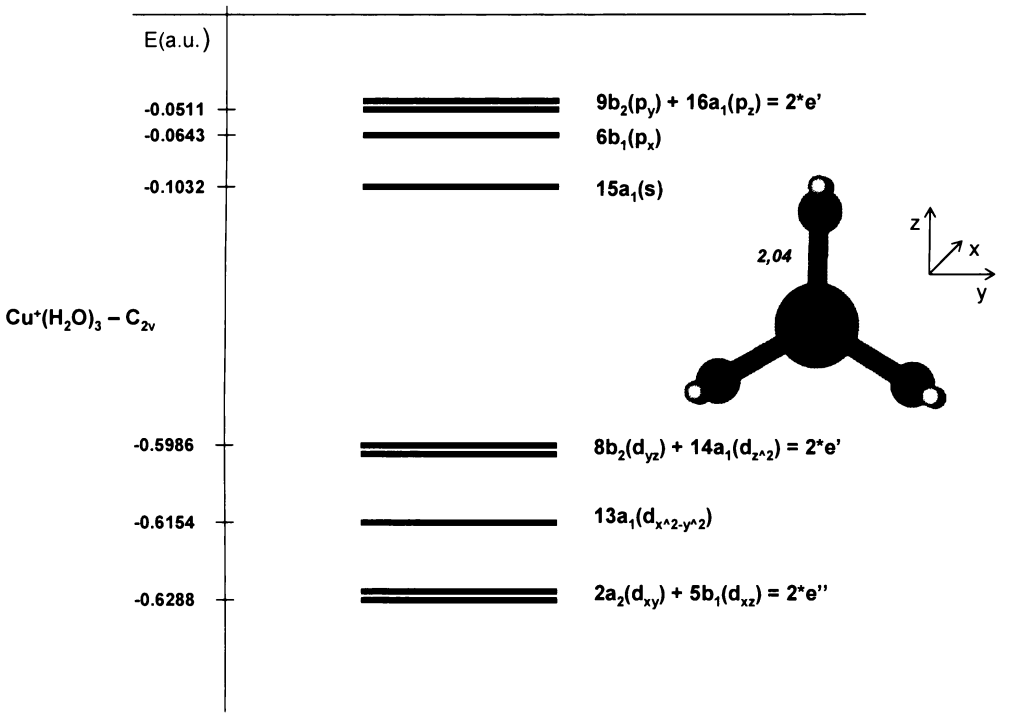

Figure 5. HF orbital diagram with the corresponding irreducible representation assignments and orbital energies, the singlet-optimized structures of cluster model $Cu^{+}(H_2O)_3$-C_{2v}.

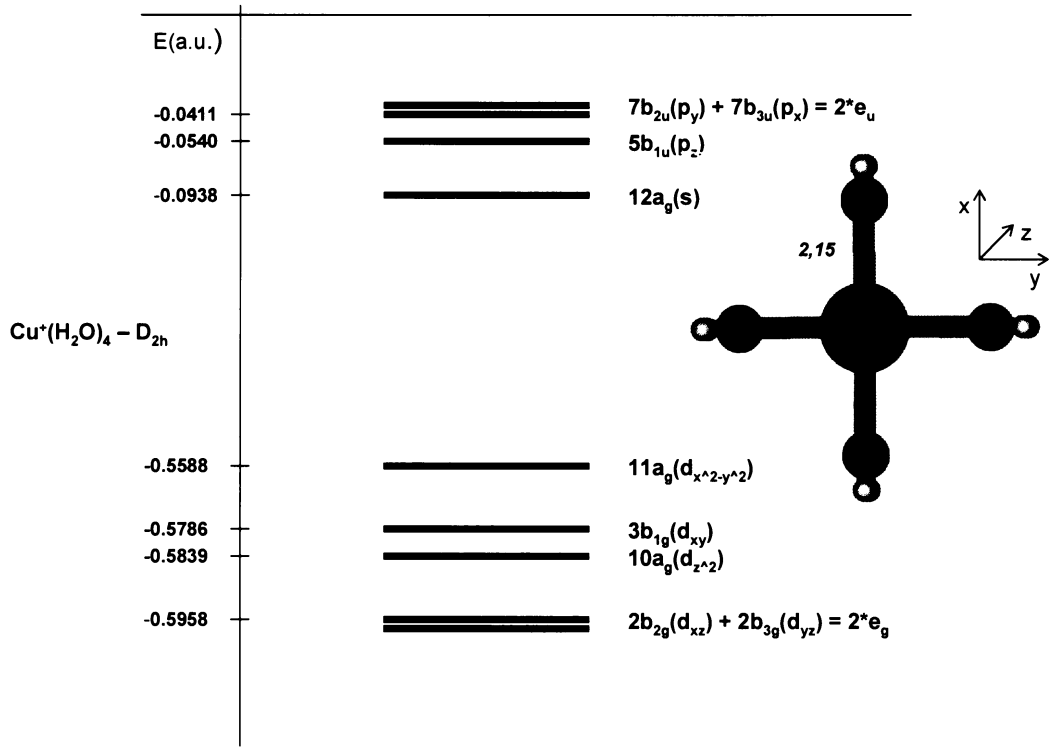

Figure 6. HF orbital diagram with the corresponding irreducible representation assignments and orbital energies, the singlet-optimized structures of cluster model $Cu^{+}(H_2O)_4$-D_{2h}.

Firstly, the HF-orbital diagrams were analyzed (see Figures 3-6), out of which four energetically least demanding excitations (one in each symmetry) were chosen for a triplet and singlet excited state computation. These excitations can be assigned to transition from 3d orbitals (a_1, b_1, b_2, a_2 and a_g, b_{1g}, b_{2g}, b_{3g} in C_{2v} and D_{2h} symmetries, respectively) to 4s (a_1 and a_g in C_{2v} and D_{2h} symmetry, respectively) orbital on Cu. Following triplet and singlet excited states were considered:

$^1A_1$, $^1A_2$, $^1B_1$, $^1B_2$, $^3A_1$, $^3A_2$, $^3B_1$, $^3B_2$, for $Cu^{+}(H_2O)_2 - C_{2v}$, $Cu^{+}(H_2O)_3 - C_{2v}$

^1A_g, $^1B_{1g}$, $^1B_{2g}$, $^1B_{3g}$, ^3A_g, $^3B_{1g}$, $^3B_{2g}$, $^3B_{3g}$, for $Cu^{+}(H_2O)_2 - D_{2h}$, $Cu^{+}(H_2O)_4 - D_{2h}$

In case of $Cu^{+}(H_2O)_3 - C_{2v}$, the consideration of both $^{1,3}A_1$ and $^{1,3}B_2$ is just an artifact of the descent in symmetry from D_{3h} to C_{2v} where E' irreducible representation transforms to $A_1 + B_2$. Thus, just one of $^{1,3}A_1$ or $^{1,3}B_2$ is taken into account. The same stands for $^{1,3}A_2$ and $^{1,3}B_1$ states which are derived from $^{1,3}E''$ state. Similarly, in the case of $Cu^{+}(H_2O)_4 - D_{2h}$ descending from D_{4h} to D_{2h} where B_{2g} and B_{3g} in D_{2h} represent the E_g in D_{4h}.

4.2 Vertical excitation energies of model systems

The vertical $T_1 \leftarrow S_0$ excitation energies were calculated as the energy difference between the lowest-energy triplet in each symmetry and ground state singlet at singlet-optimized geometry. The results are summarized in Table 2, where the lowest vertical $T_1 \leftarrow S_0$ excitation energies for each model system are in bold:

Table 2. Cluster models, excited states of corresponding symmetry, and the vertical $T_1 \leftarrow S_0$ excitation energies (in eV) computed at CCSD(T), DFT/B3LYP and DFT/PBE levels.

		$E(T_1 \leftarrow S_0)$		
Cluster model	excited state	CCSD(T)	B3LYP	PBE
$Cu^+(2H_2O)_2$ - C_{2v}	A_1	2.930	2.673	2.973
	A_2	3.012	2.753	2.894
	B_1	2.948	2.703	2.865
	B_2	**2.566**	**2.275**	**2.467**
$Cu^+(2H_2O)_2$ - D_{2h}	**A_g**	**4.050**	**3.742**	**3.983**
	B_{1g}	4.735	4.522	4.893
	B_{2g}	4.410	4.069	4.105
	B_{3g}	4.713	4.482	4.850
$Cu^+(3H_2O)_3$ - C_{2v}	$A_1 = B_2$	3.840	3.424	3.467
	$A_2 = B_1$	4.366	4.087	4.406
$Cu^+(4H_2O)_4$ - D_{2h}	**A_g**	**3.429**	**2.997**	**3.080**
	B_{1g}	-	3.596	3.637
	$B_{2g} = B_{3g}$	4.226	3.968	4.289

Similarly, the vertical $S_1 \leftarrow S_0$ excitation energies were calculated as the energy difference between the first excited singlet state and ground state singlet both at ground-state singlet optimized geometry. This procedure was carried out in each symmetry except for A_1 and A_g states in C_{2v} and D_{2h}, respectively (see Table 3).

Table 3. Cluster models, excited states of corresponding symmetry, the vertical $T_1 \leftarrow S_0$ excitation energies (in eV) computed at CCSD(T) and AQCC levels, and vertical $S_1 \leftarrow S_0$ excitation energies (in eV) computed at AQCC level.

		$E(T_1 \leftarrow S_0)$		$E(S_1 \leftarrow S_0)$
Cluster model	excited state	CCSD(T)	AQCC	AQCC
$Cu^+(2H_2O)_2 - C_{2v}$	A_1	2.930	2.907	-
	A_2	3.012	3.003	3.327
	B_1	2.948	2.937	3.303
	B_2	**2.566**	**2.577**	**2.963**
$Cu^+(2H_2O)_2 - D_{2h}$	**A_g**	**4.050**	**4.007**	**-**
	B_{1g}	4.735	4.707	5.154
	B_{2g}	4.410	4.421	4.665
	B_{3g}	4.713	4.671	4.932
$Cu^+(3H_2O)_3 - C_{2v}$	$A_1 = B_2$	3.840	3.897	-
	$A_2 = B_1$	4.366	4.364	4.661
$Cu^+(4H_2O)_4 - D_{2h}$	**A_g**	**3.429**	**3.527**	**-**
	B_{1g}	-	3.994	4.214
	$B_{2g} = B_{3g}$	4.226	4.240	4.544

4.3 Vertical excitation energies in ZSM-5 zeolite

In order to assess the possible exploitation of the data obtained in the study of realistic and more complicated systems the vertical $T_1 \leftarrow S_0$ excitation energies of three different Cu^+ sites (see Figure 7) in ZSM-5 zeolite were computed (see Table 4).

Table 4. Vertical excitation energies for various Cu^+ sites in ZSM-5 with Al located at T12[ref] (in eV)

Cu^+ sites	$E(T_1 \leftarrow S_0)$	$E(S_1 \leftarrow S_0)$[a]
I2	2.20	2.70
M6	3.62	4.02
Z8	4.12	4.52

[a] Excitation energies calculated with PBE functional and corrected for (i) PBE/CCSD(T) difference and (ii) S_1/T_1 gap (see Discussion for details)

For this task the DFT approach has been adopted employing the PBE functional. The Cu^+ sites in ZSM-5 contain the same structural patterns as the studied cluster models (see

Figure 7). The O-Cu bond lengths are depicted in Figure 7 and the O-Cu-O angle is 81.8°, 142.2° and 164,5° for I2, M6 and Z8 site, respectively.

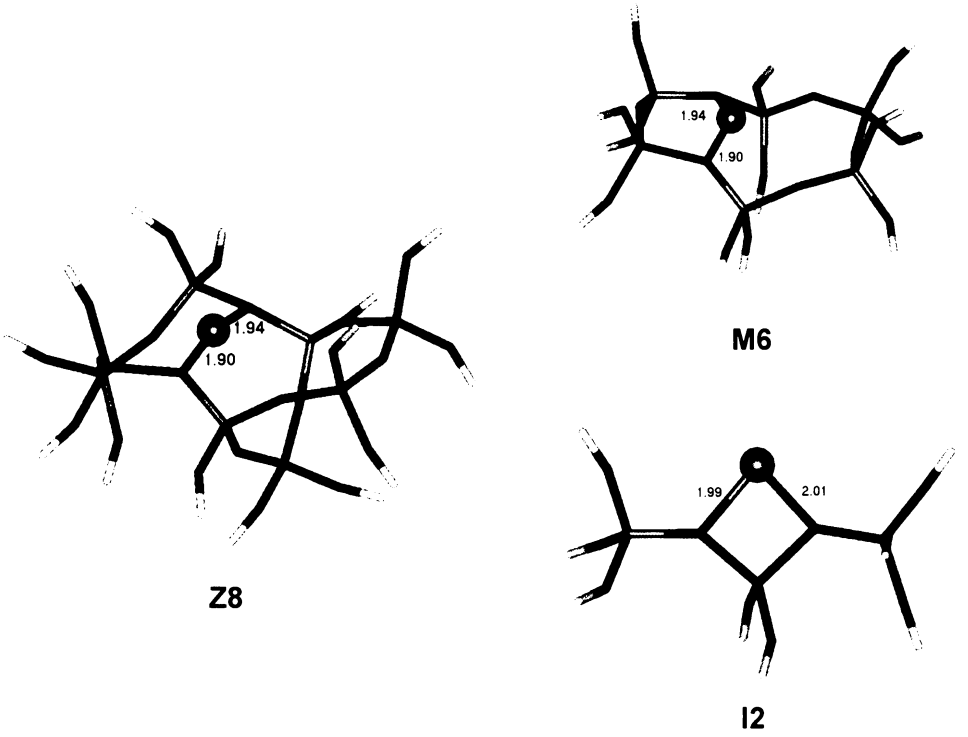

Figure 7. The I2, M6 and Z8 Cu^{+} sites in ZSM-5 zeolite (Al in T12 position). The Cu-O bond lengths (Å) are also depicted. Cu, pink circle; Al, black; Si, gray; O, red; H, white.

5. Discussion

Our study focuses on comparison of the performance of different DFT functionals (PBE, B3LYP) versus benchmark CCSD(T). Thus, enabling us to choose the proper functional depending on the studied system and the computed properties, *e.g.*, the vertical excitation energies in zeolites. The comparison also enables us to introduce the corrections for the DFT values of computed properties with respect to benchmark method, eventually the experiment, resulting in a possibility to obtain a more accurate data using a computationally less demanding method. The property chosen for the comparison in our study was the vertical excitation energy.

5.1 CCSD(T) vs. B3LYP

The data show that the difference between the vertical excitation energies obtained using CCSD(T) and DFT/B3LYP is within 0.5 eV for all the systems considered and that B3LYP tends to underestimate the vertical excitation energy. The difference of the CCSD(T) and B3LYP vertical energies slightly increases with the size of the system ranging from 0.24-0.29 eV for the $Cu^+(H_2O)_2$ - C_{2v} to 0.26-0.43 eV for $Cu^+(H_2O)_4$ - D_{2h}. While the B3LYP and CCSD(T) vertical energies corresponding to individual triplet states of the system considered vary, *e.g.*, by 0.25-0.29 eV for $Cu^+(H_2O)_2$ - C_{2v}, the variance of the difference between B3LYP and CCSD(T) vertical energies of the corresponding triplet states is within 0.05 eV. The same narrow variance of the difference between the vertical energies applies to other systems. This means that the gap between the vertical energies of the corresponding triplet states computed at CCSD(T) is preserved (see Figure 8). The fact that B3LYP is consistent with the CCSD(T) results considering the state order according to the vertical energy values is another important characteristic of B3LYP.

5.2 CCSD(T) vs. PBE

The difference of the vertical excitation energies is within 0.4 eV. The dependence of the difference of the CCSD(T) and B3LYP vertical energies on the size of the system is not observed. That is partially due to a broad variance of the vertical energies difference corresponding to triplet states of the individual system. The variance spans from 0.14 eV for $Cu^+(H_2O)_2$ - C_{2v} to 0.46 eV for $Cu^+(H_2O)_2$ - D_{2h} (see Figure 8). While some vertical energies are overestimated (the highest overestimation by 0.16 eV - $^3B_{1g}$ of $Cu^+(H_2O)_2$ - D_{2h}), the other are underestimated (the highest underestimation by 0.305 eV - $^3A_1$ of $Cu^+(H_2O)_3$ - C_{2v}) (see Figure 8). The consistency of the state order is contained except for $Cu^+(H_2O)_2$ - C_{2v} where the state order A_1, B_1, A_2 is exchanged for B_1, A_2, A_1.

5.3 B3LYP vs. PBE

The comparison of B3LYP and PBE vertical energies shows that PBE is in better agreement with CCSD(T) values than B3LYP, e.g., for the lowest triplet state by 0,2 and 0,25 eV of $Cu^+(H_2O)_2$ - C_{2v} and $Cu^+(H_2O)_2$ - D_{2h}, respectively and by 0,04 and 0,08 eV of $Cu^+(H_2O)_3$ - C_{2v} and $Cu^+(H_2O)_4$ - D_{2h}, respectively. On the other hand B3LYP contains both the state order and the gap between the vertical energies of the corresponding triplet states computed at CCSD(T). The PBE fails to reproduce the gap and in one case even to contain the state order (see Figure 8).

5.4 CCSD(T) vs. AQCC

The AQCC vertical $T_1 \leftarrow S_0$ excitation energies are in very good agreement with CCSD(T) energies varying by less then 0.1 eV being either underestimated or overestimated. The order of the states is preserved.

The AQCC vertical $S_1 \leftarrow S_0$ excitation energies are lower by 0.22-0.45 eV than $T_1 \leftarrow S_0$ energies depending on the system considered. State order set by $T_1 \leftarrow S_0$ energies is contained in $S_1 \leftarrow S_0$ energies calculations and the variation in $S_1 \leftarrow S_0$ energies for excited states belonging to different irreducible representation is 0.06, 0.2 and 0.08 eV of $Cu^+(H_2O)_2$ - C_{2v}, $Cu^+(H_2O)_2$ - D_{2h} and $Cu^+(H_2O)_4$ - D_{2h}, respectively. While the variation

in $S_1 \leftarrow S_0$ energies is small it is possible to compute the $S_1 \leftarrow S_0$ energies from the $T_1 \leftarrow S_0$ energies by simple adding a system-optimized correction to the $T_1 \leftarrow S_0$ energy value. This is an important finding for the calculations on large systems (as zeolites) since it poses a computational advantage to calculate only triplet states.

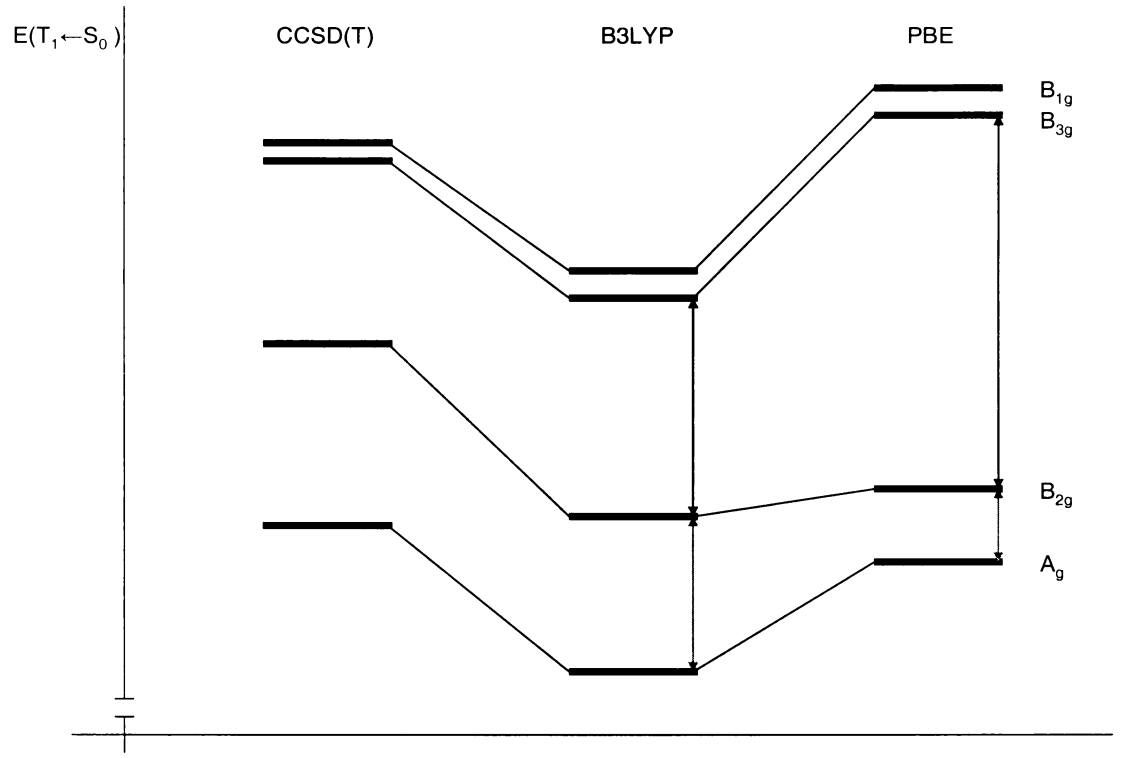

Figure 8. The diagram of the vertical $T_1 \leftarrow S_0$ excitation energies of $Cu^+(H_2O)_2$ - D_{2h} obtained by CCSD(T), DFT/B3LYP and DFT/PBE. The lines connect the excitation energies corresponding to the same triplet state.

5.5 Dependence of vertical excitation energy on the system size

A significant increase of vertical energy of 1.5 eV between the lowest – energy triplet states of $Cu^+(H_2O)_2$ - C_{2v} and $Cu^+(H_2O)_2$ - D_{2h} is observed. The observation can be explained as the consequence of the Cu(4s) orbital occupation resulting from 3d → 4s excitation. As the spatial extent of the Cu(4s) is large the significant repulsive interactions with lone-pair electrons on oxygen atoms occur. In case of $Cu^+(H_2O)_2$ - C_{2v} there is a possibility to form a hybridized sp orbital (4s and $4p_z$ belong to the same irreducible representation). Hence, the electron density is redistributed and moved away

from the lone-pairs on oxygen atoms. Thus, the repulsive interactions are reduced which results in lowering the excitation energy compared to $Cu^+(H_2O)_2$ - D_{2h}.

Going from $Cu^+(H_2O)_2$ - D_{2h} to $Cu^+(H_2O)_4$ - D_{2h} vertical excitation energy of the lowest-energy triplet state decreases by 0.6 eV. In order to explain the trend two aspects need to be evaluated. One is the repulsive interaction of Cu(4s) orbital with lone-pair electrons on oxygen atoms which rises with the size of the system as more lone-pair electrons are involved but lowers with the increasing bond length (see Figures 3-6). The other effect is the repulsion interaction of oxygen atoms with the highest occupied Cu(3d) orbital oriented towards these neighboring oxygen atoms which increases with the size of the system. To get the qualitative picture of the discussed repulsion interactions it is possible to consider the HOMO – LUMO gap where HOMO energy represents Cu(3d) repulsion with oxygen atoms while LUMO energy Cu(4s) repulsive interaction with lone-pair orbitals. The LUMO and HOMO energies are in line with prediction as both LUMO and HOMO energies increase with the increasing size of the system (see Figures 3-6). As the increase in energy is more significant for the HOMO the gap narrows for the larger systems what results in observed vertical energy decrease.

5.6 The ZSM-5 zeolite vs. cluster model vertical excitation energies

Looking at the parameters (the Cu-O bond length and O-Cu-O angle) of the Cu^+ sites in ZSM-5 versus the parameters of the cluster models one can notice a close resemblance of both Cu^+ sites and cluster models. The I2 site is similar to $Cu^+(H_2O)_2$ - C_{2v} (angle the same, bond length shorter by 0.5 Å), Z8 to $Cu^+(H_2O)_2$ - D_{2h} (angle differs by 15°, bond within 0.05 Å) while M6 is a halfway between the $Cu^+(H_2O)_2$ - C_{2v} and $Cu^+(H_2O)_2$ - D_{2h}.

Our study shows that the values of the vertical $T_1 \leftarrow S_0$ excitation energies are in line with the observed structural resemblance since they increase going from I2 to Z8 as well as going from $Cu^+(H_2O)_2$ - C_{2v} to $Cu^+(H_2O)_2$ - D_{2h}. The difference of the $T_1 \leftarrow S_0$ energies (the lowest-energy triplet state is considered) between I2 site and $Cu^+(H_2O)_2$ - C_{2v} is 0.25 eV while for the Z8 site and it is only 0.15 eV what can be explained as a consequence of higher similarity of Z8 site and $Cu^+(H_2O)_2$ - D_{2h} compared to I2 site and $Cu^+(H_2O)_2$ - C_{2v}.

In case of $S_1 \leftarrow S_0$ vertical excitation energies the experimental data for ZSM-5 are available. While the Cu^+ sites are, as previously discussed, structurally similar to the cluster models (this holds not only for the $Cu^+(H_2O)_2$ - C_{2v} and $Cu^+(H_2O)_2$ - D_{2h} with two coordinated oxygen atoms but for highly coordinated $Cu^+(H_2O)_3$ - C_{2v} and $Cu^+(H_2O)_4$ - D_{2h} as well)[5] the comparison of the calculated $S_1 \leftarrow S_0$ vertical excitation energies is at hand. Based on the EXAFS, IR and photoluminescence data, Lamberti et al. suggested that two types of Cu^+ sites exist in ZSM-5, characterized by the 300 nm (4.1 eV) and 256 nm (4.9 eV) peaks in the excitation photoluminescence spectra.[9] The $S_1 \leftarrow S_0$ vertical excitation energies for the Cu^+ sites in ZSM-5 are obtained by correcting the calculated DFT/PBE vertical $T_1 \leftarrow S_0$ excitation energies (see Table 4). The correction of 0.1 eV (the lowest-energy triplet state of $Cu^+(H_2O)_2$ - C_{2v} is considered) is due to PBE underestimation of $T_1 \leftarrow S_0$ excitation energy compared to CCSD(T) value (see Table 2 and paragraph 5.2). Another corrections of 0.4 eV for I2 site and 0.3 eV for M6 and Z8 sites arise from the $T_1 \leftarrow S_0$ vs. $S_1 \leftarrow S_0$ splitting as it is assumed to be approximately constant (see paragraph 5.4 and Table 4). Thus, the predictions for the $S_1 \leftarrow S_0$ vertical excitation energies are lower by 1.4 eV for I2 site but just by 0.1 eV for M6 site than the observed band maxima at 4.1 eV and lower by 0.4 eV for Z8 site compared to the observed maxima at 4.9 eV. The difference between the predicted $S_1 \leftarrow S_0$ vertical excitation energies and experimental data can be explained as a consequence of the fact that the excitation energies observed in the spectra correspond to the electronic transition often accompanied with vibrational transitions (see Figure 2 – Franck-Condon effects). Besides the energy increase due to vibrational transitions, the excitation to the higher-energy singlet states resulting in energy increase can occur. Hence, the experimental excitation energy is higher than the predicted $S_1 \leftarrow S_0$ vertical excitation energy. We may conclude that the two well-separated peaks correspond to different Cu^+ sites in ZSM-5, the higher-energy peak at 256 nm to Z8 type of site while the lower-energy peak at 300 nm to M6 type of site. The presence of the I2 type of site in ZSM-5 is not observed.

7. Conclusions

The comparison of the performance of the DFT method employing both B3LYP and PBE exchange-correlation functionals versus the benchmark CCSD(T) method have been obtained. The PBE values of the lowest vertical excitation energies for the studied cluster models are in better agreement with CCSD(T) values than B3LYP. However for the higher excited states, the PBE is unable to contain the gap between the vertical energies of the corresponding triplet states computed at CCSD(T) and in some cases even to reproduce the energy order of the triplet states while the B3LYP contains both the gap (the B3LYP values are shifted compared to the CCSD(T)) and the state order. We may conclude that the PBE is a better option for calculation of the lowest-energy triplet state. In order to get a better general description of the excitations the B3LYP is the method of choice. The difference between the DFT and CCSD(T) excitation energies is relatively constant, thus, the DFT values can be easily corrected.

The calculations of the vertical $T_1 \leftarrow S_0$ excitation energies as well as the vertical $S_1 \leftarrow S_0$ excitation energies have been carried out using the AQCC method. The AQCC vertical $T_1 \leftarrow S_0$ excitation energies are in a very good agreement with CCSD(T) energies deviating by less then 0.1 eV. As for the AQCC vertical $S_1 \leftarrow S_0$ excitation energies the difference between the $T_1 \leftarrow S_0$ and $S_1 \leftarrow S_0$ values for the different triplet states is almost constant what enables the introduction of the correction to the previously computed $T_1 \leftarrow S_0$ excitation energies, thus, resulting in the reduction of vertical $S_1 \leftarrow S_0$ excitation energy calculation time.

The vertical $T_1 \leftarrow S_0$ excitation energies for the Cu^+ sites in the ZSM-5 zeolite (I2, M6, Z8), which are structurally similar to studied cluster models, have been calculated as well. The corrections derived from the previous comparisons made on the cluster models were used for the calculation of the vertical $S_1 \leftarrow S_0$ excitation energies. The predicted vertical $S_1 \leftarrow S_0$ excitation energies are 2.7, 4.0 and 4.5 eV for I2, M6 and Z8 site, respectively. The experimental data from the excitation photoluminescence spectra provide two peaks in range 3.9-4.5 (the band maxima at 4.1 eV) and 4.5-5.2 eV (the band maxima at 4.9 eV). Thus, the comparison of the predicted $S_1 \leftarrow S_0$ excitation energies with

the experimental data suggest the presence of two Cu^{+} sites (M6, Z8) in the ZSM-5 while the presence of I2 type of site is not supported.

Reference List

1. Iwamoto, M.; Furukawa, H.; Mine, Y.; Uemura, F.; Mikuriya, S. I.; Kagawa, S. Copper(Ii) Ion-Exchanged Zsm-5 Zeolites As Highly-Active Catalysts for Direct and Continuous Decomposition of Nitrogen Monoxide. *Journal of the Chemical Society-Chemical Communications* **1986,** (16), 1272-1273.

2. Iwamoto, M.; Hamada, H. Removal of nitrogen monoxide from exhaust gases through novel catalytic processes. *Catalysis Today* **1991,** *10* (1), 57-71.

3. Iwamoto, M.; Yahiro, H. Novel Catalytic Decomposition and Reduction of No. *Catalysis Today* **1994,** *22* (1), 5-18.

4. Teraishi, K.; Ishida, M.; Irisawa, J.; Kume, M.; Takahashi, Y.; Nakano, T.; Nakamura, H.; Miyamoto, A. Active site structure of Cu/ZSM-5: Computational study. *Journal of Physical Chemistry B* **1997,** *101* (41), 8079-8085.

5. Nachtigallova, D.; Nachtigall, P.; Sierka, M.; Sauer, J. Coordination and siting of Cu+ ions in ZSM-5: A combined quantum mechanics interatomic potential function study. *Physical Chemistry Chemical Physics* **1999,** *1* (8), 2019-2026.

6. Dedecek, J.; Wichterlova, B. Siting and Redox Behavior of Cu Ions in Cuh-Zsm-5 Zeolites - Cu+ Photoluminescence Study. *Journal of Physical Chemistry* **1994,** *98* (22), 5721-5727.

7. Wichterlova, B.; Dedecek, J.; Vondrova, A. Identification of Cu Sites in Zsm-5 Active in No Decomposition. *Journal of Physical Chemistry* **1995,** *99* (4), 1065-1067.

8. Yamashita, H.; Matsuoka, M.; Tsuji, K.; Shioya, Y.; Anpo, M.; Che, M. In-situ XAFS, photoluminescence, and IR investigations of copper ions included within various kinds of zeolites. Structure of Cu(I) ions and their interaction with CO molecules. *Journal of Physical Chemistry* **1996,** *100* (1), 397-402.

9. Lamberti, C.; Bordiga, S.; Salvalaggio, M.; Spoto, G.; Zecchina, A.; Geobaldo, F.; Vlaic, G.; Bellatreccia, M. XAFS, IR, and UV-vis study of the Cu-I environment in Cu-I-ZSM-5. *Journal of Physical Chemistry B* **1997,** *101* (3), 344-360.

10. Møller, C.; Plesset, M. S. Note on an Approximation Treatment for Many-Electron Systems. *Phys. Rev.* **1934,** *46* (7), 618.

11. Cizek, J. On Correlation Problem in Atomic and Molecular Systems . Calculation of Wavefunction Components in Ursell-Type Expansion Using Quantum-Field Theoretical Methods. *Journal of Chemical Physics* **1966,** *45* (11), 4256-&.

12. Meyer, W. Pno-Ci Studies of Electron Correlation Effects .1. Configuration Expansion by Means of Nonorthogonal Orbitals, and Application to Ground-State and Ionized States of Methane. *Journal of Chemical Physics* **1973,** *58* (3), 1017-1035.

13. Ahlrichs, R.; Lischka, H.; Staemmler, V.; Kutzelnigg, W. Pno-Ci (Pair Natural Orbital Configuration Interaction) and Cepa-Pno (Coupled Electron Pair Approximation with Pair Natural Orbitals) Calculations of Molecular Systems .1. Outline of Method for Closed-Shell States. *Journal of Chemical Physics* **1975,** *62* (4), 1225-1234.

14. Kutzelnigg, W.; Shaefer, H. F. *Methods of Electronic Structure Theory;* Plenum: New York, 1977.

15. Ahlrichs, R.; Scharf, P.; Ehrhardt, C. The Coupled Pair Functional (Cpf) - A Size Consistent Modification of the Ci(Sd) Based on An Energy Functional. *Journal of Chemical Physics* **1985,** *82* (2), 890-898.

16. Gdanitz, R. J.; Ahlrichs, R. The Averaged Coupled-Pair Functional (Acpf) - A Size-Extensive Modification of Mr Ci(Sd). *Chemical Physics Letters* **1988,** *143* (5), 413-420.

17. Szalay, P. G.; Bartlett, R. J. Multireference Averaged Quadratic Coupled-Cluster Method - A Size-Extensive Modification of Multireference Ci. *Chemical Physics Letters* **1993,** *214* (5), 481-488.

18. Szalay, P. G.; Muller, T.; Lischka, H. Excitation energies and transition moments by the multireference averaged quadratic coupled cluster (MR-AQCC) method (vol 2, pg 2067, 2000). *Physical Chemistry Chemical Physics* **2001,** *3* (11), 2190.

19. Hohenberg, P.; Kohn, W. Inhomogeneous Electron Gas. *Physical Review B* **1964,** *136* (3B), B864-&.

20. Kohn, W.; Sham, L. J. Self-Consistent Equations Including Exchange and Correlation Effects. *Phys. Rev.* **1965,** *140* (4A), 1133-&.

21. Perdew, J. P.; Burke, K.; Ernzerhof, M. Generalized gradient approximation made simple. *Physical Review Letters* **1996,** *77* (18), 3865-3868.

22. Perdew, J. P.; Burke, K.; Ernzerhof, M. Generalized gradient approximation made simple (vol 77, pg 3865, 1996). *Physical Review Letters* **1997,** *78* (7), 1396.

23. Becke, A. D. Density-Functional Thermochemistry .3. the Role of Exact Exchange. *Journal of Chemical Physics* **1993,** *98* (7), 5648-5652.

24. Becke, A. D. Density-Functional Exchange-Energy Approximation with Correct Asymptotic-Behavior. *Physical Review A* **1988,** *38* (6), 3098-3100.

25. Lee, C. T.; Yang, W. T.; Parr, R. G. Development of the Colle-Salvetti Correlation-Energy Formula Into A Functional of the Electron-Density. *Physical Review B* **1988,** *37* (2), 785-789.

26. Runge, E.; Gross, E. K. U. Density-Functional Theory for Time-Dependent Systems. *Physical Review Letters* **1984,** *52* (12), 997-1000.

27. Emrich, K. An Extension of the Coupled Cluster Formalism to Excited-States .1. *Nuclear Physics A* **1981,** *351* (3), 379-396.

28. Emrich, K. An Extension of the Coupled Cluster Formalism to Excited-States .2. Approximations and Tests. *Nuclear Physics A* **1981,** *351* (3), 397-438.

29. Sekino, H.; Bartlett, R. J. A Linear Response, Coupled-Cluster Theory for Excitation-Energy. *International Journal of Quantum Chemistry* **1984,** 255-265.

30. Schafer, A.; Horn, H.; Ahlrichs, R. Fully Optimized Contracted Gaussian-Basis Sets for Atoms Li to Kr. *Journal of Chemical Physics* **1992,** *97* (4), 2571-2577.

31. Dunning, T. H. Gaussian-Basis Sets for Use in Correlated Molecular Calculations .1. the Atoms Boron Through Neon and Hydrogen. *Journal of Chemical Physics* **1989,** *90* (2), 1007-1023.

32. Bergner, A.; Dolg, M.; Kuchle, W.; Stoll, H.; Preuss, H. Ab-Initio Energy-Adjusted Pseudopotentials for Elements of Groups 13-17. *Molecular Physics* **1993,** *80* (6), 1431-1441.

33. Gaussian 03, Revision C.02, Frisch, M. J.; Trucks, G. W.; Schlegel, H. B.; Scuseria, G. E.; Robb, M. A.; Cheeseman, J. R.; Montgomery, Jr., J. A.; Vreven, T.; Kudin, K. N.; Burant, J. C.; Millam, J. M.; Iyengar, S. S.; Tomasi, J.; Barone, V.; Mennucci, B.; Cossi, M.; Scalmani, G.; Rega, N.; Petersson, G. A.; Nakatsuji, H.; Hada, M.; Ehara, M.; Toyota, K.; Fukuda, R.; Hasegawa, J.; Ishida, M.; Nakajima, T.; Honda, Y.; Kitao, O.; Nakai, H.; Klene, M.; Li, X.; Knox, J. E.; Hratchian, H. P.; Cross, J. B.; Bakken, V.; Adamo, C.; Jaramillo, J.; Gomperts, R.; Stratmann, R. E.; Yazyev, O.; Austin, A. J.; Cammi, R.; Pomelli, C.; Ochterski, J. W.; Ayala, P. Y.; Morokuma, K.; Voth, G. A.; Salvador, P.; Dannenberg, J. J.; Zakrzewski, V. G.; Dapprich, S.; Daniels, A. D.; Strain, M. C.; Farkas, O.; Malick, D. K.; Rabuck, A. D.; Raghavachari, K.; Foresman, J. B.; Ortiz, J. V.; Cui, Q.; Baboul, A. G.; Clifford, S.; Cioslowski, J.; Stefanov, B. B.; Liu, G.; Liashenko, A.; Piskorz,

P.; Komaromi, I.; Martin, R. L.; Fox, D. J.; Keith, T.; Al-Laham, M. A.; Peng, C. Y.; Nanayakkara, A.; Challacombe, M.; Gill, P. M. W.; Johnson, B.; Chen, W.; Wong, M. W.; Gonzalez, C.; and Pople, J. A.; Gaussian, Inc., Wallingford CT, 2004. 2004.

34. Werner, H. J.; Knowles, P. J. MOLPRO 02. 2002.

35. Nachtigall, P.; Nachtigallova, D.; Sauer, J. Coordination change of Cu+ sites in ZSM-5 on excitation in the triplet state: Understanding of the photoluminescence spectra. *Journal of Physical Chemistry B* **2000,** *104* (8), 1738-1745.